PL-TR-97-2167

SMALL ON-BOARD ENVIRONMENTAL DIAGNOSTIC SENSORS PACKAGE (SOBEDS)

Bronislaw K. Dichter
Marilyn R. Oberhardt
John O. McGarity
Robert Redus
Wallie Everest
Alan Donkin
Valentin Jordanov
John A. Pantazis
Alan C. Huber

AMPTEK, INC.
6 De Angelo Drive
Bedford, MA 01730-2204

9 December 1997

Scientific Report No. 2

APPROVED FOR PUBLIC RELEASE; DISTRIBUTION UNLIMITED

AIR FORCE RESEARCH LABORATORY
Space Vehicles Directorate
29 Randolph Road
AIR FORCE MATERIEL COMMAND
HANSCOM AFB, MA 01731-3010

This Scientific Report #2 has been reviewed and is approved for publication.

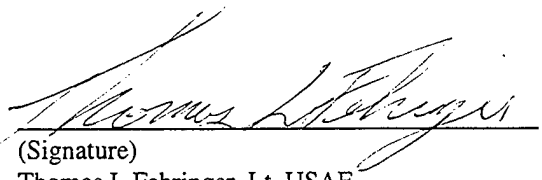

(Signature)
Thomas L Fehringer, Lt, USAF
Contract Manager

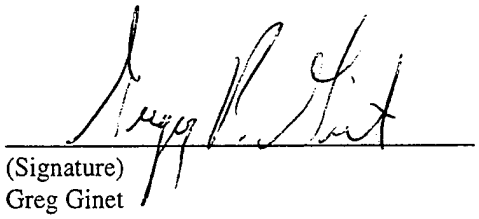

(Signature)
Greg Ginet
Branch Chief

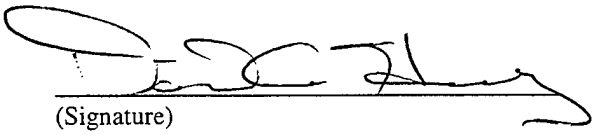

(Signature)
Dave Hardy
Division Director

This report has been reviewed by the ESC Public Affairs Office (PA) and is releasable to the National Technical Information Service (NTIS).

Qualified requestors may obtain additional copies from the Defense Technical Information Center (DTIC). All others should apply to the National Technical Information Service (NTIS).

If your address has changed, if you wish to be removed from the mailing list, or if the addressee is no longer employed by your organization, please notify AFRL/VSOS-IM, 29 Randolph Road, Hanscom AFB, MA 01731-3010. This will assist us in maintaining a current mailing list.

Do not return copies of this report unless contractual obligations or notices on a specific document require that it be returned.

REPORT DOCUMENTATION PAGE

Form Approved
OMB No. 0704-0188

1. AGENCY USE ONLY *(Leave blank)*	2. REPORT DATE	3. REPORT TYPE AND DATES COVERED
	12/9/1997	Scientific No. 2

4. TITLE AND SUBTITLE

Small On-Board Environmental Diagnostics Sensors Package (SOBEDS)

5. FUNDING NUMBERS

PE 63410F
PR 2822 TA GC WU AM

Contract F19628-95-C-0227

6. AUTHOR(S)

Bronislaw K. Dichter, Robert Redus, Valentin Jordanov
John O. McGarity, Wallie Everest, John A. Pantazis
Marilyn R. Oberhardt, Alan Donkin, Alan C. Huber

7. PERFORMING ORGANIZATION NAME(S) AND ADDRESS(ES)

AMPTEK, Inc.
6 De Angelo Drive
Bedford, MA 01730

8. PERFORMING ORGANIZATION REPORT NUMBER

9. SPONSORING / MONITORING AGENCY NAME(S) AND ADDRESS(ES)

Air Force Research Laboratory
29 Randolph Road
Hanscom AFB, MA 01731-3010

Contract Manager: Lt. Tom Fehringer/VSBS

10. SPONSORING / MONITORING AGENCY REPORT NUMBER

PL-TR-97-2167

11. SUPPLEMENTARY NOTES

12a. DISTRIBUTION / AVAILABILITY STATEMENT

Approved for public release; distribution unlimited

12b. DISTRIBUTION CODE

13. ABSTRACT *(Maximum 200 words)*

The Small On-Board Environmental Sensors Package (SOBEDS) is a suite of spacecraft instruments designed to measure ionizing radiation in the near-Earth space environment. The purpose of data gathered by the SOBEDS instrument is to improve the understanding of the Earth's radiation belts and the effect of ionizing radiation on Air Force space systems. This report is concerned with the experimental and computational effort in the design of the High Energy Proton (HEP) sensor for the SOBEDS suite. HEP is designed to measure the differential energy fluxes of protons with energies between 25 and 300 MeV.

14. SUBJECT TERMS

Spacecraft Radiation Measurement, Electrons, Protons, Dosimetry

15. NUMBER OF PAGES

20

16. PRICE CODE

17. SECURITY CLASSIFICATION OF REPORT	18. SECURITY CLASSIFICATION OF THIS PAGE	19. SECURITY CLASSIFICATION OF ABSTRACT	20. LIMITATION OF ABSTRACT
Unclassified	Unclassified	Unclassified	SAR

Table of Contents

Table of Figures

List of Tables

1 INTRODUCTION

This report contains the summary of the scientific and engineering work performed as part of the development of the High Energy Proton instrument (HEP). HEP is a part of the SOBEDS suite of instruments being developed by Amptek, Inc. The purpose of the HEP instrument is to detect incident high energy protons ($15 \leq E \leq 300$ MeV) and measure their energy spectrum.

The primary technical effort during the second year of the SOBEDS contract has been devoted to the manufacture and testing of the Engineering Model HEP sensor head. The key issue in this effort was the characterization of the response of the scintillator materials which are to be used as the primary proton detector in the HEP instrument. Four scintillator materials were extensively studied: GSO (Gd_2SiO_5), LuAP ($LuAlO_3$), BGO ($Bi_4Ge_3O_{12}$) and PWO ($PbWO_4$). The testing work was carried out with radioactive sources at Amptek, Inc. and with proton beams at two accelerators, Harvard Cyclotron (HCL) and the Alternating Gradient Synchrotron (AGS) at the Brookhaven National Laboratory (BNL).

A description of the HEP Engineering Sensor head and of the experimental setups at HCL and AGS is contained in Section 2. The sensor head proton response, both measured and calculated, is described in Section 3. A discussion of the sensor head response to high energy proton induced nuclear interactions is in Section 4. Finally, a summary of the work and concluding remarks are in Section 5.

2 EXPERIMENTAL HARDWARE AND SETUPS

2.1 HEP Sensor Head

An engineering model (EM) of the HEP sensor head was manufactured for the purpose of testing the key hardware components and data handling algorithms intended for use with the flight instrument. A cross section diagram of the EM sensor head is shown in Figure 1. The design allowed a flexibility in accommodating the evaluation of a variety of scintillator materials and scintillator light readout devices.

There are five detection elements in the EM, two scintillators and three solid state detectors. The two scintillators are labeled S1 and S2 in Figure 1. The mechanical design allowed any

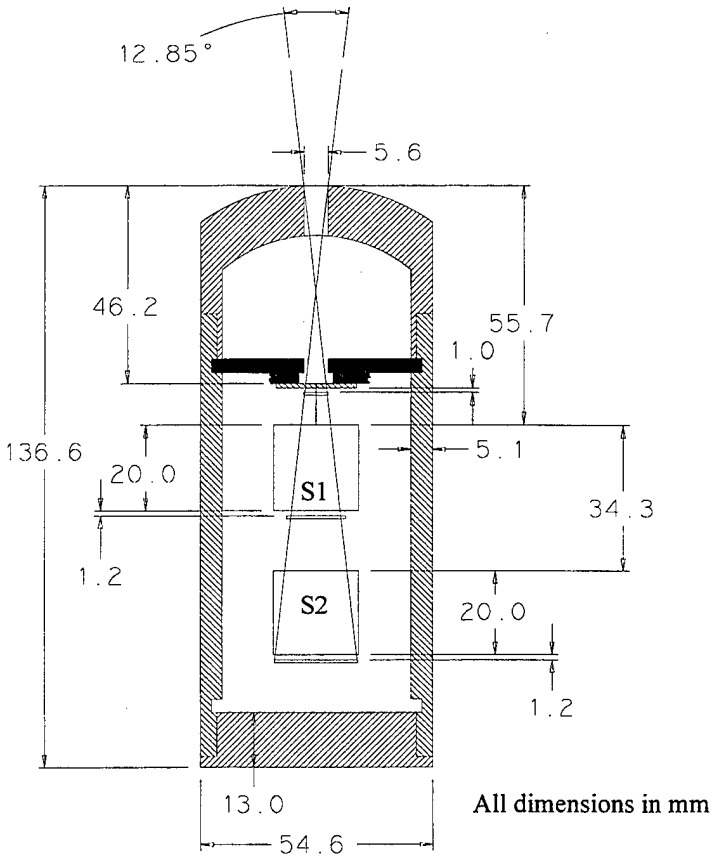

Figure 1. Cross section diagram of the HEP EM sensor head.

cylindrical scintillator 2 cm long and 2 cm in diameter to be placed in the sensor head. The three solid state detectors (D1, D3 and D4) are all 700 μm thick and had areas of 0.25, 1.5 and 3.0 cm^2, respectively. D1 is located between the EM entrance aperture and S1, D3 is between S1 and S2 and D4 is located between S2 and the rear shield. A 0.1 cm thick Cu degrader disk is located in the entrance aperture upstream of D1, preventing the lowest energy particles from reaching the EM detectors. The scintillation light from S1 and S2 could be detected by either photomultiplier tubes (PMT) or by photodiodes, depending on the EM configuration. The EM sensors are surrounded by a Cu shield, 1.3 cm at the front and back and 0.5 cm along the sides.

2.2 External Electronics and Data Acquisition System

The EM sensor head does not include any internal electronics. All signal processing is performed by external electronic modules, both custom designed and commercial NIM electronics. Similarly, data acquisition from the sensor is performed by an external, Amptek Inc. designed, system consisting both of commercial components (CAMAC crate and PC) and custom software. The use of external electronics permitted the work on the sensor head to proceed independently and in parallel to the work on the development of HEP flight electronics.

The readout of the scintillation light produced in S1 and S2 was accomplished using the circuit shown in
Figure 2. The scintillator was wrapped with a diffuse reflector (Teflon tape) except where it was coupled to the PMT through a quartz light guide. The scintillation light was collected onto the PMT photocathode and the resulting electron pulse was amplified by the PMT high voltage electrode chain. The output current pulse from the PMT was coupled, using a 50 Ω terminator, to the input of an Ortec 450 main amplifier (Int. = 0.1 μsec, Diff. = OUT). The unipolar Ortec 450 output was sent, through a delay amplifier, to the data acquisition system's analog-to-digital converter, ADC (Ortec AD811). The bipolar output signal was converted to a negative NIM logic pulse by the Ortec 551 TSCA module and then sent to the data acquisition system's counter/scaler (LRS 2551).

The readout of the solid state detectors (D1, D3 and D4) was accomplished using a circuit identical to the D1 circuit shown in Figure 3. The output signal from each detector was first

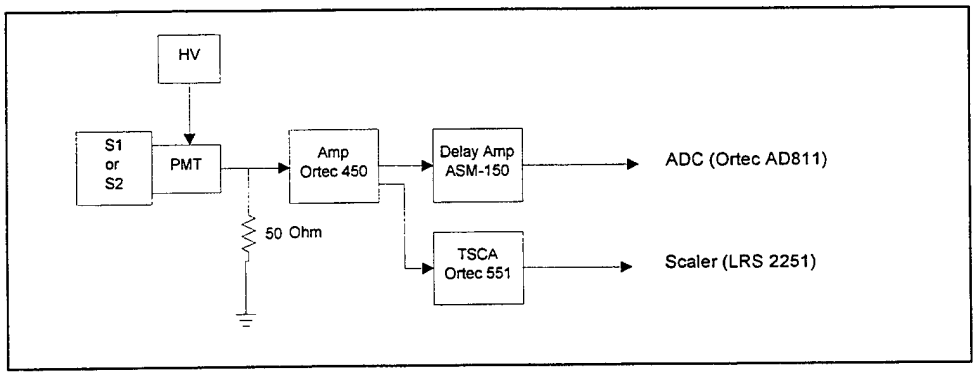

Figure 2. Block diagram of the scintillator readout electronics.

processed by custom built pre-amplifier/amplifier module (ASM-200), based on the Amptek A-225 hybrid. The slow, shaped ASM-200 output (2 μsec time constant) was sent to the ADC after a suitable delay. The fast ASM-200 output was converted to a positive NIM logic pulse by the Ortec 551 TSCA module and the resulting pulse was used as one of the inputs to an Ortec 418A Coincidence unit.

There were five inputs to the Coincidence module: D1, D3, D4, a beam monitor solid state detector (M2) (see Section 2.3) and a time-of-flight (TOF) telescope signal (see Section 2.4). The unit could be configured to accept any combination of these five signals, including singles counts from any sensor, as a valid event. For a valid event, the Coincidence unit generated a logic signal which gated the AD811 CAMAC ADC. Thus, unless a preset coincidence requirement was met the ADC did not digitize any signals. Once a valid event occurred, the ADC performed pulse height analysis on all (up to eight) of its input signals.

The CAMAC scaler (LRS 2251) was used to count the beam induced events in all of the sensor head detectors (S1, S2, D1, D3 and D4), the beam monitor detectors (M1 and M2), and the TOF telescope (AGS only, see Section 2.4). In addition, the total number of valid events, as determined by the Coincidence unit, was also counted by the LRS 2251. The count rates from the 100 MHz, free-running scaler were free of the dead time that affected the CAMAC ADC data (80 μsec AD811 digitization time and PC SCSI communications overhead) and were used to correct for the dead time related undercounting of valid events.

The HEP beam experiments were controlled by a two computer network (see Figure 4). PC#1 ran the data acquisition program HEPDAQ, which communicated with the CAMAC crate using a SCSI card. PC#1 also ran another program which communicated with the motion control system using the PC-38 card, supplied by the motion system manufacturer. HEPDAQ polled the CAMAC crate for valid events accepted by the AD811. If such an event (receipt of a gate from the Coincidence unit by the AD811) occurred, HEPDAQ would 1) transfer the digitized pulse

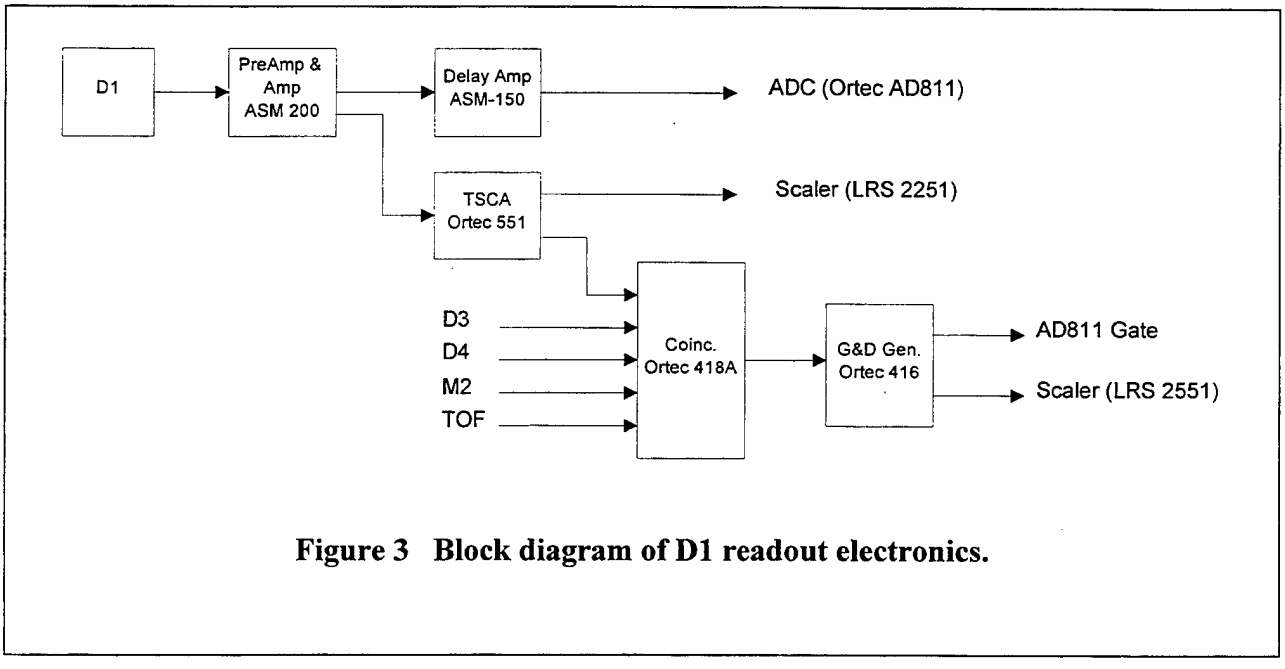

Figure 3 Block diagram of D1 readout electronics.

height data for that event from the AD811 to PC#1, 2) clear the old data from the AD811 and 3) enable the AD811 to accept the next event. After every 250 events processed by HEPDAQ, the program would read and clear the data from the LRS 2251 scaler.

HEPDAQ stored the data retrieved on an event-by-event basis from the AD8911 and the LRS 2251 in a disk file on PC#1. In order to free up the PC#1 system resources for CAMAC communications, HEPDAQ performed no data analysis and was strictly a data retrieval and storage program. PC#2 ran the data analysis and display program. This program would periodically access the data file written on PC#1 by HEPDAQ, perform simple analysis on the data and update the various displayed spectra and scaler counts.

The motion control system included one rotary and two linear stages. The EM sensor head was mounted on top of the rotary stage, which in turn was attached to a linear stage. This configuration allowed the EM to be both moved perpendicularly to the beam and to be rotated with respect to the beam axis. One of the solid state beam monitor detectors (M2) was mounted on the second, independent linear stage (referred to as Monitor Stage in Figure 4). This allowed M2 to be placed in the beam line and directly up stream of the EM, whenever desired by the experimenter.

2.3 Experimental Setup at HCL

The cyclotron at HCL produces a 160 MeV proton beam. The beam exits the vacuum environment of the accelerator through a thin pressure window and enters the room where the experiment is performed. Just downstream of the window, the beam is directed through a 3.2 cm diameter collimator. Several calibrated degrader plugs (made of lead and Lexan) can be inserted

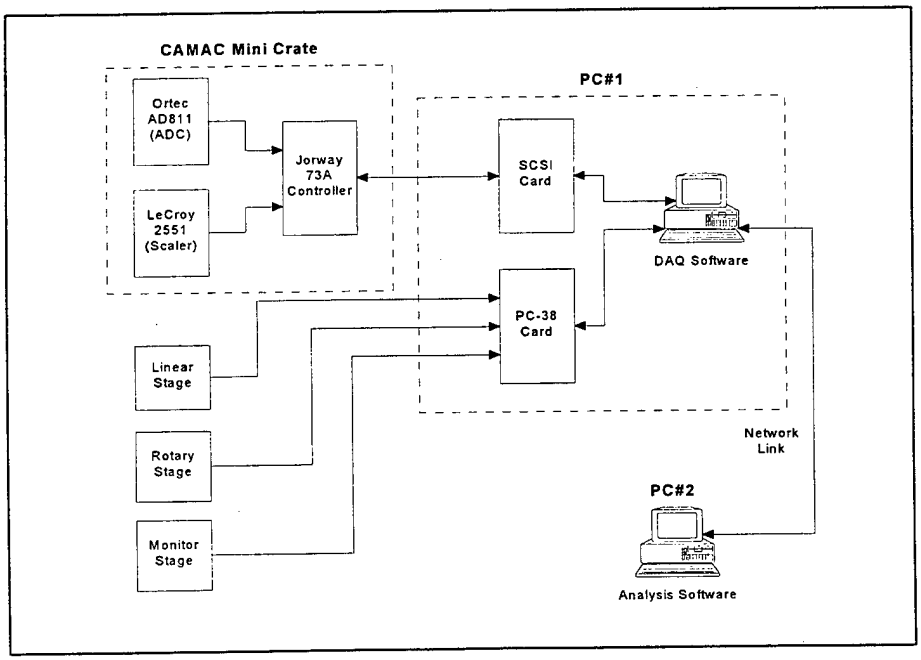

Figure 4. Block diagram of the experiment control system.

into the collimator tunnel to decrease the incident beam energy. The standard degrader set produces the following mean energies at the exit of the collimator: 29, 37, 45, 54, 73, 92, 111, 131 and 149 MeV. The EM sensor head was located 165 cm downstream of the collimator.

There were two beam monitor detectors. One, with a 0.25 cm^2 area, was permanently mounted to one side of the EM entrance aperture, while the second one (0.50 cm^2 area) was mounted on a linear motion stage and could be moved into the beam line directly in front of EM aperture. When this detector was in the beam line, it was used as part of the event trigger. For example, the Coincidence unit could be configured to require simultaneous hits in the monitor detector and in D1 in order to register a valid event.

2.4 Experimental Setup at AGS

The AGS experiments were performed at the B2 Test Beam. The AGS accelerator produces a primary beam of 33 GeV protons. There are many secondary and tertiary beam lines which produce a variety of subatomic particle beams. The B2 Test Beam can be configured to provide a positively charged beam (positrons, muons, kaons, protons and deuterons) with a particle momentum range of 0.6 to 2.0 GeV/c. This range corresponds to a proton energy range of 175 to 1,280 MeV.

The B2 beam is a mixture of all types of particles, all with the same momentum. Since only the proton response of the EM sensor head is of interest, it is necessary to provide a trigger mechanism sensitive to particle type so that the proton induced events in the EM can be distinguished from those induced by other particles. The time-of-flight (TOF) telescope provides such a trigger.

The principle of operation of the TOF telescope is straightforward. The velocity of a particle is measured and the relationship between velocity and momentum is used to obtain the particle mass and, thus, its identity. The relativistic relationship between the momentum, p, of a particle and its kinetic energy, T, is given by

$$p = \sqrt{2Tmc^2 + T^2} \qquad (1)$$

where m is the particle's rest mass and c is the velocity of light. Since the momentum of all the beam particles is the same but the masses are different, each particle will have a different kinetic energy and a different velocity, v, where

$$v/c = \beta = \sqrt{1 - \frac{1}{\left(1 + \frac{T}{mc^2}\right)^2}} \qquad (2)$$

If the time-of-flight of the beam particle, TOF, is measured over a fixed distance, d, then the velocity is given by

$$v = d / TOF \ . \qquad (3)$$

Thus, a measured value of the TOF yields particle velocity, which can be converted to kinetic energy (Eq. (2)) and finally, using the known beam momentum, to mass (Eq. (1)).

The TOF telescope (loaned to us by the PHOENIX group at the AGS) consisted of two plastic scintillator detectors placed 10 m apart and located directly upstream of the EM sensor head. The TOF detectors had a larger diameter than the EM entrance aperture so that any particle striking the EM had to have hit both TOF counters. The time difference between the particle passage through the front and back TOF detectors was converted to an analog voltage pulse using the Ortec 566 time-to-amplitude (TAC) converter module (see readout circuit in Figure 5). The output of the TAC was used both as part of the valid event definition and as an input to the AD811 ADC.

Normally, the valid event trigger (from the Coincidence unit) consisted of a TOF signal from the TSCA and one or more of the D1-D4 detectors. The TOF signal from the TSCA could result from any beam particle (positrons, muons, kaons as well as protons and deuterons). In this way, events caused by all types of particles were recorded by the data acquisition system. However, since the actual TOF signal from the TAC was digitized and recorded for each event, it was possible during data analysis to select only events that had a TOF value which identified them as induced by beam protons.

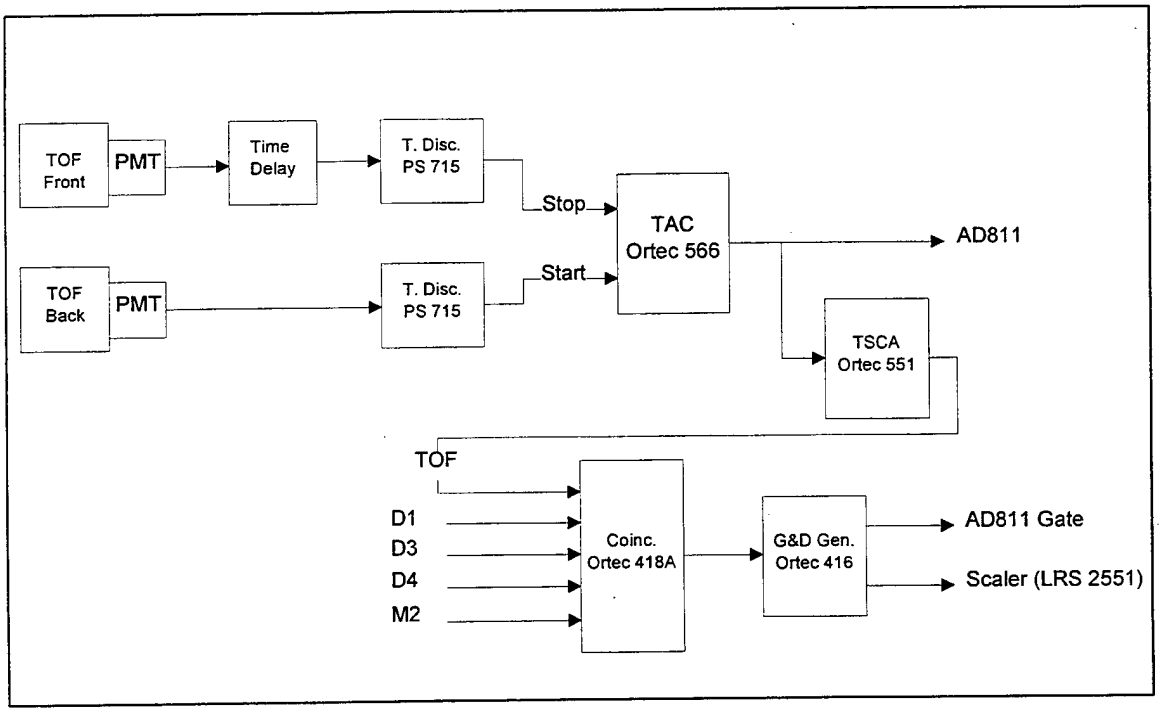

Figure 5. Block diagram of the TOF readout electronics.

3 HEP SENSOR HEAD RESPONSE TO PROTONS

3.1 Scintillator Material Comparison

The performance of the scintillator material used for S1 and S2 is the key to the proper performance of the HEP sensor. The important characteristics of a suitable material are

a) **high density**: this feature results in smaller S1 and S2 which, in turn, leads to a smaller and less massive instrument,

b) **high light output**: this feature allows the use of photodiodes instead of photomultiplier tubes to read out the S1 and S2 signals, leading to a decrease in size, power and complexity,

c) **good energy resolution**: this feature permits accurate measurement of incident proton energy, particularly for high energy protons which traverse both S1 and S2,

and

d) **fast decay time**: this feature permits maintaining good energy resolution at high count rates, an important issue for an instrument designed to work in the inner radiation belt,

Four commercially available scintillator materials were evaluated for use in the HEP instrument. The reported properties of these materials are listed in Table 1.

Table 1. Listing of reported scintillator properties (Refs. 1, 2 and 3).

Property	Material			
	LuAp	GSO	PWO	BGO
Density (g/cm^3)	8.4	6.7	8.3	7.1
Light Output (ph/MeV)	10,900	7,900	100	8,060
Energy Res. (^{137}Cs γ-ray)	9%	11%	N/A	11%
Decay Time (ns)	16	60	10	400
Peak Emission (nm)	365	430	450-530	480
Rad. Hardness (rad)	N/A	$> 10^7$	$\sim 10^6$	10^5-10^6

In the final analysis, GSO was chosen for use on HEP. The primary reasons for the rejection of the other materials were

LuAP: Poor energy resolution (20%) for high energy protons, apparently caused by the manufacturer's inability to produce material of uniform purity,

PWO: Scintillation light output insufficient for use with photodiode and poor energy resolution for high energy protons (20%),

BGO: Long decay time and poor thermal stability, both light output and decay time vary strongly with changes in temperature.

In view of this scintillator choice, only the results for GSO will be given in the remainder of this section.

3.2 GSO Scintillation Light Output

We have studied the production of scintillation light by GSO in order to verify that the HEP sensor head scintillators can be read out by photodiodes rather than require PMT for readout. The measured scintillation light output is determined by the intrinsic material properties as well as by the particulars of the crystal geometry, reflective coating, type of incident particles, system electronics and the quality of the optical coupling to the light sensor.

If $M_{e\text{-}h}$ is the number of electron-hole (e-h) pairs produced in the photodiode per MeV of energy deposited in the scintillator by high energy protons, then

$$M_{e-h} = N_\gamma \, R_{p\gamma} \, \varepsilon_{tot} \tag{4}$$

where N_γ is the number of scintillation photons produced by 662 keV γ-rays (^{137}Cs), $R_{p\gamma}$ is the scintillation light production for high energy protons relative to the 662 keV γ-rays and ε_{tot} is the probability for converting a single scintillation photon to an e-h pair. The total probability can be written as a product of three components,

$$\varepsilon_{tot} = \varepsilon_g \varepsilon_{pd} \varepsilon_e \tag{5}$$

where the ε_g is the probability of the scintillation photon striking the photodiode active area, ε_{pd} is the typical quantum efficiency of the photodiode in the wavelength region of the scintillation light and ε_e is the fraction of the total photodiode current detected by the readout electronics.

Moszynski *et al.* (Ref. 2) have studied the intrinsic light production by GSO and measured $N_\gamma = 6630 \pm 380$ and $\varepsilon_{pd} = 0.72$ for the Hamamatsu S-3950 photodiode. During the experiment at the AGS, we determined $R_{p\gamma} = 0.83$ by measuring the relative amounts of light produced in the GSO by 2 GeV/c protons (which deposited 23 MeV in a 2 cm long GSO crystal) and by 662 keV γ-rays from ^{137}Cs. The value ε_g may be estimated using the expression for the light collection

efficiency for an enclosed volume with walls of reflectivity R and a ratio f of the photo detector sensitive area to the surface area of the enclosed volume

$$\varepsilon_g \cong \frac{f}{[1-(1-f)R]} \quad . \tag{6}$$

The GSO crystal, 2 cm long and 2 cm in diameter, in combination with the small quartz light guide had an area of 22.7 cm^2. The surface area of the photodiode was 0.8 cm^2, giving f = 0.036. The crystal and light guide were wrapped with several layers of Teflon tape, with an estimated R of 0.98, resulting in $\varepsilon_g \cong 0.65$. Finally, we used a light integration time of 250 ns, which was sufficient to collect all of the light from the short lifetime GSO decay component (τ = 60 ns) but not the long lifetime one (τ = 600 ns). Since the ratio of intensities of the two components is 7:1 (Ref. 1) our electronics missed approximately 14% of the scintillation light and $\varepsilon_e \cong 0.86$. Substituting these values into eqs. (4) and (5) gives $M_{e\text{-}h}$(calculated) = 2,215 e-h/MeV.

We measured the value of $M_{e\text{-}h}$ directly by comparing the photodiode signal generated by the passage of 2 GeV/c protons (23 MeV of deposited energy in the scintillator) with the signal generated by a direct absorption by the photodiode of the 59.5 keV γ-rays from ^{241}Am. The second case is known to generate 16,540 e-h pairs, allowing the direct calibration of deposited energy to e-h pairs for high energy protons. The measured value of $M_{e\text{-}h}$ is 1,405 e-h/MeV. Given the uncertainties in the estimation of the various efficiencies and the fact the N_γ value from Ref. 2 was obtained with a GSO crystal made by a different manufacturer than the one used in the present work, the agreement between the measured and calculated values is satisfactory.

3.3 GSO Proton Response: Measurements and Computations

Average energy loss by charged particles in matter is described by the Bethe-Block equation. An extensive discussion of this equation and tabulations of stopping power, dE/dx, and range for protons in various elements and compounds is found in Ref. 4. The scintillator materials considered for use in this program are relatively new and are not listed in the Tables of Ref. 4. Therefore, some additional computation was required to obtain the needed information for these materials.

The stopping power of a compound, $(dE/dx)_C$ may be computed from the stopping power of its constituent elements by making the assumption that the stopping power per atom is additive (Bragg-Kleeman rule):

$$\left(\frac{dE}{dx}\right)_C = N_C \sum_i \frac{W_i}{N_i}\left(\frac{dE}{dx}\right)_i \tag{7}$$

where N is the atomic density, dE/dx is the stopping power and W_i is the fraction of atoms of element i in the compound (subscript c). In practice, the right hand side of Eq. (7) must be multiplied by a constant k, which accounts for any compound effects on stopping power and any

inaccuracies in tabulated elemental stopping powers. We found that a value of k = 1.05 works well with all the heavy scintillator compounds studied.

In addition to the analytical energy loss calculations using the Bethe-Block equation, we have undertaken a series of Monte Carlo simulations of the response of the HEP sensor head to high energy protons using the HETC code (Ref. 5). This code follows the history of each incident proton, on an "event-by-event" basis, as it traverses the sensor head, interacting with the sensor head electrons and nuclei. This allows us to obtain extremely detailed information about the distribution of energy loss values in the sensor head detectors. This is in contrast to the Bethe-Block calculations which result in the computation of average values only. In addition, the HETC code realistically treats the effects of nuclear interactions in the HEP detectors (see Section 4).

The experiments carried out at HCL and the AGS resulted in the measurement of the incident proton energy loss distributions in S1 and S2. These distributions were, in general, characterized by a well defined peak in the deposited energy spectra for the two scintillators. The measured peak positions and the energy loss curves computed using the Bethe-Block equation, Eq. (7), are shown in Figure 6. The error bars on the data points correspond to the measured full-width-at-half-maximum (FWHM) of the energy deposition peaks.

A comparison of the measured energy loss values with the values calculated with 1) the Bethe-Block equation and 2) the Monte Carlo HETC program is shown in Figure 7. The plotted points are the ratios of the calculated energy loss values to the measured ones for the S1 scintillator. It is clear that there is a systematic deviation of about 5% for both calculations from

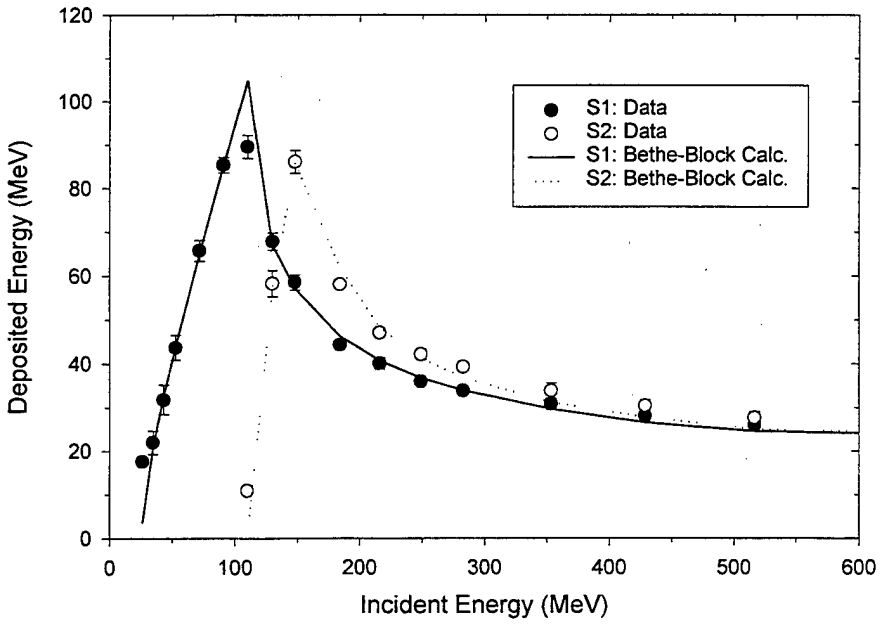

Figure 6. Computed energy loss in S1 and S2 scintillators.

the measured data points. Once this effect is taken into account, the agreement between data and calculation is excellent. The 5% deviation is well within the size of the errors expected by using the Bragg-Kleeman approximation to compute the stopping power of an actual compound.

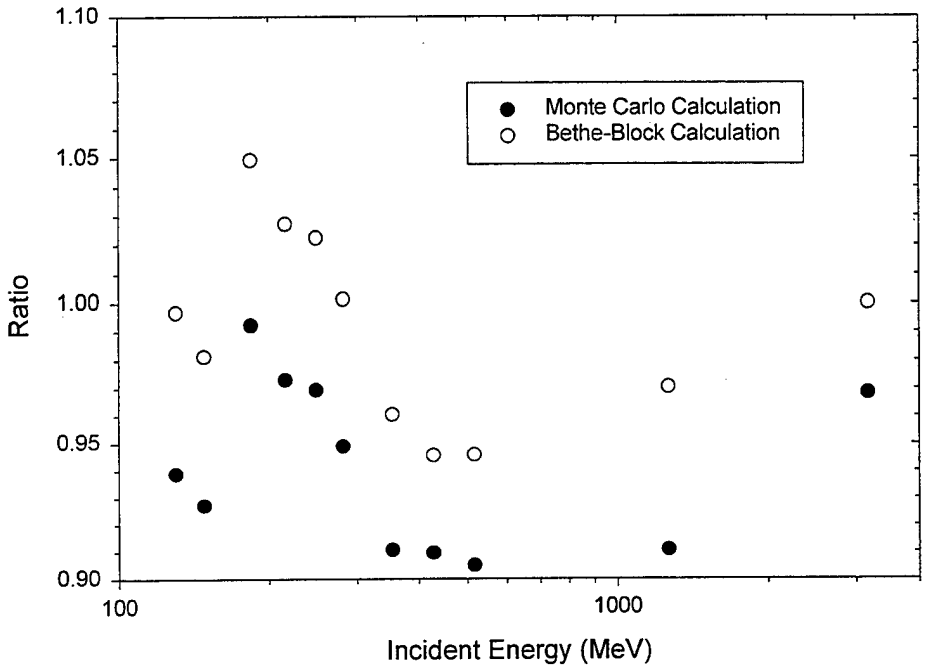

Figure 7. Ratio of calculated to measured proton energy losses in S1.

4 HEP SENSOR HEAD RESPONSE TO NUCLEAR INTERACTIONS

The HEP sensor response to protons must be corrected for the effect of nuclear interactions between high energy protons and the atoms of the scintillator material. These events result in very large energy deposition in either S1 or S2 scintillator. This causes the instrument electronics to reject nuclear interaction events from processing. The final effect is to reduce the measured proton flux by the fraction of the total events that result in nuclear interactions.

The probability of a nuclear interaction may be estimated using the following simple geometrical model. In order for a nuclear interaction to take place, the incident proton must overcome the repulsive Coulomb barrier, B_C, of the target nucleus and approach within a distance, R_C, where the proton comes in physical contact with the target nucleons. The Coulomb barrier is given by

$$B_C = \frac{Z_1 Z_2 e^2}{R_C} \tag{8}$$

where the Coulomb radius, is approximately given by

$$R_C = [\,1.12\,(A_1^{1/3} + A_2^{1/3}) - 0.94\,(A_1^{-1/3} + A_2^{-1/3}) + 3\,]\ fm \tag{9}$$

where A_1 and A_2 are the atomic numbers of the incident and target nucleus and R_C is in units of fm (10^{-15} m). In this model, the total reaction cross section, σ_R, cannot exceed the area of a disk with a radius of R_C, and can be written as

$$\sigma_R = \pi R_C^2 \left(\frac{E - B_C}{E} \right) \cong \pi R_C^2 \qquad for\ E >> B_C \tag{10}$$

where E is the incident particle energy. The proton energies used in the experiments were well above the B_C values for the elements that make up GSO: 2 MeV for oxygen, 3 MeV for silicon and 10 MeV for gadolinium. Thus, the condition $E >> B_C$ is satisfied and the limiting value of σ_R can be used. The interaction probability, P_n, is then

$$P_n = N t \sigma_R \tag{11}$$

where N is the atomic density of the target material and t is the target thickness. In case of a compound material, like GSO, σ_R is the sum of the atomic cross sections for all the atoms of the molecule. Evaluating Eq. (11) for a 2 cm long GSO crystal yields $P_n = 0.20$. Similarly, $P_n = 0.004$ for a D1 or D2 detector and $P_n = 0.014$ for a 1 mm thick copper degrader located upstream of the D1 detector.

The output of the Monte Carlo HETC code permits the selection of events which result in very large energy deposition in one area of the sensor head. These events are due to nuclear

interactions. The HETC probabilities for these events are 0.077 ± 0.010 for S1, 0.082 ± 0.009 for S2, 0.0012 ± 0.0008 for D1, 0.0015 ± 0.0011 for D2 and 0.0049 ± 0.0017 for the copper degrader (the errors are due to counting statistics in the Monte Carlo simulation). The simple geometrical model predicts 2.5 times the number of nuclear interactions predicted by HETC. This is a reasonable result, given that Eq. (11) counts all nuclear interactions, most of which result in only small energy releases due to the knock out of a small number of nucleons, while the HETC events are only those that result in massive energy deposition.

The experimental configurations used at HCL and the AGS precluded us from directly observing nuclear interaction events in the HEP sensor head. We plan on altering the configuration during the next phase of beam measurements to be able to observe these events. This will allow us to determine the accuracy of the HETC nuclear interaction predictions.

5 SUMMARY AND CONCLUSIONS

We have performed extensive experimental and computational work to characterize the response of the HEP sensor head to protons. The experiments utilized high energy proton beams and were performed at the Harvard Cyclotron Laboratory ($30 < E < 148$ MeV) and at the AGS accelerator at the Brookhaven National Laboratory ($184 < E < 1{,}270$ MeV). The computational work was carried out using a variety of approaches, including the HETC Monte Carlo code. The overall agreement between experimental data and the calculation results is excellent, suggesting that the HEP sensor head simulations are accurate. We are now using results of the simulation work to further refine the sensor head design.

6 REFERENCES

1 . V. V. Avdeichkov, L Bergholt, M. Guttormsen, J. E. Taylor, L. Westerberberg, B. Jakobsson, W. Klamra and Yu. A. Murin, "Light output and energy resolution of CsI, YAG, GSO, BGO and LSO scintillators for light ions", NIM **A349**, pp. 216-224, 1994.

2. M. Moszynski, M. Kapusta, M. Mayhugh, D. Wolski and S. O. Flyck, "Absolute light output of scintillators", IEEE Trans. Nucl. Sci. Vol. 44, pp. 1052-166, 1996.

3. G. Yu. Drobyshev, A. A. Fyodorov, M. V. Korzhik, O.V. Misevich, V. A. Katchanov and J. P. Peigneux, "Optimization of a lead tungstate crystal/photodetecor system for high-energy physics", IEEE Trans. Nucl. Sci. Vol. 42, pp. 341-344.

4. J. F. Janni, Calculations of Energy Loss, Range, Pathlength, Straggling, Multiple Scattering, and the Probability of Nuclear Collisions for 0.1 to 1000 MeV Protons, AFWL-TR-65-150, 1965.

5 . HETC (High Energy Transport Code)" is a component of the "CALOR95 - Monte Carlo Program Code System", ORNL RSIC Computer Code Collection, CCC-610, Oak Ridge National Laboratory, Oct. 1996.